J. Opt. A: Pure Appl. Opt. **10** (2008) 064009 (9pp) doi:10.1088/1464-4258/10/6/064009

The Virgo 3 km interferometer for gravitational wave detection

F Acernese[1], P Amico[2], M Alshourbagy[3], F Antonucci[4], S Aoudia[5], P Astone[4], S Avino[1], L Baggio[6], G Ballardin[7], F Barone[1], L Barsotti[3], M Barsuglia[8], Th S Bauer[9], S Bigotta[3], M A Bizouard[8], C Boccara[10], F Bondu[5], L Bosi[2], C Bradaschia[3], J F J van den Brand[9], S Birindelli[3], S Braccini[3], A Brillet[5], V Brisson[8], D Buskulic[6], G Cagnoli[11], E Calloni[1], E Campagna[11], F Carbognani[7], F Cavalier[8], R Cavalieri[7], G Cella[3], E Cesarini[11], E Chassande-Mottin[5], A-C Clapson[8], F Cleva[5], E Coccia[12], C Corda[3], A Corsi[4], F Cottone[2], J-P Coulon[5], E Cuoco[7], S D'Antonio[12], A Dari[2], V Dattilo[7], M Davier[8], M del Prete[3], R De Rosa[1], L Di Fiore[1], A Di Lieto[3], A Di Virgilio[3], B Dujardin[5], M Evans[7], V Fafone[12], I Ferrante[3], F Fidecaro[3], I Fiori[7], R Flaminio[6,7], J-D Fournier[5], S Frasca[4], F Frasconi[3], L Gammaitoni[2], F Garufi[1], E Genin[7,14], A Gennai[3], A Giazotto[3,7], L Giordano[1], V Granata[6], C Greverie[5], D Grosjean[6], G Guidi[11], S Hamdani[7], S Hebri[7], H Heitmann[5], P Hello[8], D Huet[7], S Kreckelbergh[8], P La Penna[7], M Laval[5], N Leroy[8], N Letendre[6], B Lopez[7], M Lorenzini[11], V Loriette[10], G Losurdo[11], J-M Mackowski[13], E Majorana[4], C N Man[5], M Mantovani[3], F Marchesoni[2], F Marion[6], J Marque[7], F Martelli[11], A Masserot[6], F Menzinger[7], L Milano[1], Y Minenkov[12], C Moins[7], J Moreau[10], N Morgado[13], S Mosca[1], B Mours[6], I Neri[2], F Nocera[7], G Pagliaroli[12], G V Pallottino[4], C Palomba[4], F Paoletti[3,7], S Pardi[1], A Pasqualetti[7], R Passaquieti[3], D Passuello[3], F Piergiovanni[11], L Pinard[13], R Poggiani[3], M Punturo[2], P Puppo[4], S van der Putten[9], P Rapagnani[4], T Regimbau[10], V Reita[10], A Remillieux[13], F Ricci[4], I Ricciardi[1], A Rocchi[12], R Romano[1], P Ruggi[7], G Russo[1], S Solimeno[1], A Spallicci[5], M Tarallo[3], R Terenzi[12], M Tonelli[3], A Toncelli[3], E Tournefier[6], F Travasso[2], C Tremola[3], G Vajente[3], D Verkindt[6], F Vetrano[11], A Viceré[11], J-Y Vinet[5], H Vocca[2] and M Yvert[6]

[1] INFN, Sezione di Napoli and/or Università di Napoli 'Federico II' Complesso Universitario di Monte S Angelo, Italia and/or Università di Salerno, Fisciano (Sa), Italy
[2] INFN Sezione di Perugia and/or Università di Perugia, Perugia, Italy
[3] INFN, Sezione di Pisa and/or Università di Pisa, Pisa, Italy
[4] INFN, Sezione di Roma and/or Università 'La Sapienza', Roma, Italy
[5] Departement Artemis—Observatoire Cote d'Azur, BP 42209, F-06304 Nice, Cedex 4, France
[6] Laboratoire d'Annecy-le-Vieux de Physique des Particules (LAPP), IN2P3/CNRS, Université de Savoie, Annecy-le-Vieux, France
[7] European Gravitational Observatory (EGO), Cascina (Pi), Italy
[8] LAL, Université Paris-Sud, IN2P3/CNRS, Orsay, France
[9] NIKHEF, NL-908 DB Amsterdam and/or Vrije Universiteit, NL-971 HV Amsterdam, The Netherlands
[10] ESPCI, Paris, France
[11] INFN, Sezione di Firenze/Urbino, Sesto Fiorentino, and/or Università di Firenze, and/or Università di Urbino, Italy
[12] INFN, Sezione di Roma Tor Vergata and/or Università di Roma Tor Vergata, Roma, Italy
[13] LMA, Villeurbanne, Lyon, France

E-mail: eric.genin@ego-gw.it

Received 29 October 2007, accepted for publication 9 January 2008
Published 1 May 2008
Online at stacks.iop.org/JOptA/10/064009

[14] Address for correspondence: European Gravitational Observatory, Traversa H di via Macerata, I-56021 Cascina, Italy.

Abstract

Virgo, designed, constructed and developed by the French–Italian VIRGO collaboration located in Cascina (Pisa, Italy) and aiming to detect gravitational waves, is a ground-based power recycled Michelson interferometer, with 3 km long suspended Fabry–Perot cavities. The first Virgo scientific data-taking started in mid-May 2007, in coincidence with the corresponding LIGO detectors.

The optical scheme of the interferometer and the various optical techniques used in the experiment, such as the laser source, control, alignment, stabilization and detection strategies are outlined.

The future upgrades that are planned for Virgo from the optical point of view, especially concerning the evolution of the Virgo laser, are presented.

Finally, the next generation of the gravitational wave detector (advanced Virgo) is introduced from the point of view of the laser system.

Keywords: gravitational waves, laser, interferometer, Michelson

(Some figures in this article are in colour only in the electronic version)

1. Introduction

The Virgo detector is a Michelson interferometer with 3 km long Fabry–Perot cavities in its arms. Built by a French–Italian collaboration, its aim is the detection of gravitational waves [1]. The instrument is located near Pisa in Italy. Of all of the ground-based detectors, Virgo has been designed to have the best sensitivity in the low frequency region thanks to the particular seismic attenuators from which the mirrors are suspended. After the end of construction (Summer 2003), and a very intensive commissioning phase, a first scientific data-taking period began in May 2007 and lasted for four and a half months.

The apparatus is designed to achieve a relative spectral displacement sensitivity of better than $\delta l/l = 10^{-21}$ Hz$^{-1/2}$ between 20 Hz and 10 kHz. The sensitivity will be limited by seismic disturbances below 3 Hz, by thermal noise up to 100 Hz and by shot noise for higher frequencies.

In order to reach this extreme sensitivity, the Virgo detector uses special techniques to minimize the coupling of noise into the interferometric signal. The large optics (mirrors and beamsplitters) are super-polished fused silica pieces with very low absorption and scattering (bulk absorption <1 ppm cm^{-1}; coating absorption <5 ppm). They are located in an ultra-high vacuum system and suspended from a sophisticated seismic isolation system, the so-called superattenuator, which offers very high passive isolation [2]. However, the motion at the resonance frequencies of this system (from 10 mHz to 4 Hz) can be large and must be reduced by active control.

To guarantee stable long-term operation and a high sensitivity the angular degrees of freedom have to be actively controlled.

In this paper, the optical scheme of the interferometer, the laser system and the strategy of control are described.

The future evolution of Virgo in order to improve the detector sensitivity, particularly the laser system, is also presented.

Finally, an introduction to the next-generation gravitational wave detector is given.

2. Principle of operation

Figure 1 shows a simplified optical layout of the Virgo interferometer in the recycled configuration.

The laser light, 20 W @1064 nm provided by an injection locked master–slave solid state laser (Nd:YVO_4), enters the vacuum system at the suspended injection bench (SIB). The beam is spatially filtered by a 144 m long input mode cleaner cavity (IMC) before being injected into the main interferometer.

The laser frequency is pre-stabilized, using the input mode cleaner cavity length as a reference, by an analogue electronic loop. The low-frequency stability is achieved by an additional control system that stabilizes the input mode cleaner length below 15 Hz to the length of a so-called reference cavity (RFC), a 30 cm long rigid triangular cavity. Once the interferometer is locked, the laser frequency stabilization loop (second-stage frequency stabilization: SSFS) is engaged in order to further improve the laser frequency stability by using the interferometer common mode.

A beam with 10 W of power enters the Michelson interferometer through the power-recycling mirror.

It is split into two beams that are injected into the 3 km long arm cavities. The finesse of the arm cavities is approximately 50. The flat input mirrors and the spherical end mirrors form a stable resonator with the beam waist at the input mirrors having a radius of approximately 21 mm. The power reflected by the interferometer is recycled by the power recycling mirror, which creates a new optical cavity that enables a reduction of the shot noise by a factor of $\sim$7 and an improvement of the sensitivity of the detector.

The interferometer is held on the dark fringe and the expected gravitational wave signal would be measured in the beam from the dark port, which is passed through an *output mode cleaner* (OMC), a 2.5 cm long monolithic cavity, and then detected on photodiode B1 (in fact, B1 is a group of three photodiodes).

The interferometer control systems utilize the interferometer output signals and a modulation–demodulation method.

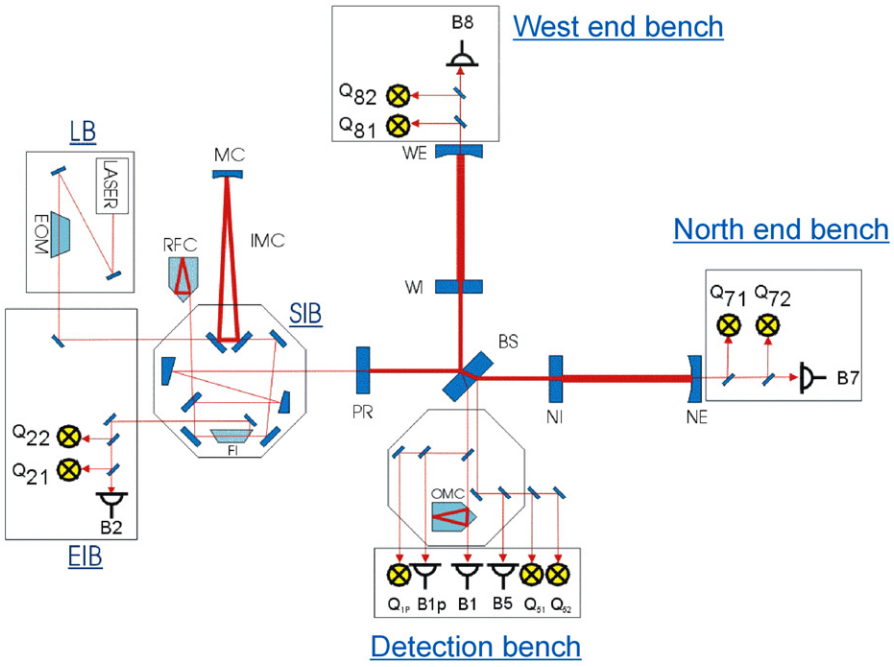

Figure 1. Scheme of the Virgo interferometer: the laser beam is directed on the *external injection bench* (EIB) into the first vacuum chamber, the injection tower, in which all optical components are attached to a suspended optical bench, the *suspended injection bench* (SIB). After passing the *input mode cleaner* (IMC), the beam is injected through the *power-recycling mirror* (PR) into the interferometer. Here, the beam is split and enters the two 3 km long arm cavities, the *west arm* and *north arm*. The Michelson interferometer is held at the dark fringe so that most of the light power is reflected back to the PR. In the final configuration the PR and the Michelson interferometer form a Fabry–Perot-like cavity in which the light power is enhanced. The light from the dark port of the *beamsplitter* is filtered by an *output mode cleaner* (OMC) before being detected on a set of photodiodes (B1), which generate the main output signal of the detector. The other photodiodes shown in this schematic with names starting with **B** are used for longitudinal control of the interferometer; diodes named with a **Q** represent quadrant photodetectors used for alignment control.

For this purpose the laser beam is modulated in phase with an electro-optic modulator (EOM, see figure 1) at $f_{\mathrm{RF}} = 6.26$ MHz.

This phase modulation generates new frequency components with a frequency offset of $\pm f_{\mathrm{RF}}$ to the frequency of the laser beam f_0. These frequency components are called *sidebands* and the light field at f_0 is called the *carrier*. The light detected by the photodiodes in several output ports of the interferometer is then demodulated with the same frequency f_{RF} or multiples of that frequency. The demodulated signals from single-element diodes (B1–B8) are used for the length control of the interferometer, whereas the demodulated signals from quadrant photodiodes (Q1p–Q82) provide control signals for the angular degrees of freedom of the interferometer mirrors.

The modulation–demodulation technique is commonly used in many interferometers, especially in the other interferometric gravitational wave detectors: LIGO (USA), TAMA (Japan) and GEO600 (GB and Germany) [3–5]. However, for each interferometer a unique control topology has been developed, depending on the details of the experimental realization of the optical system.

2.1. Locking the cavities: Pound–Drever–Hall locking technique (PDH)

In order to keep the light resonating in the cavities formed by the suspended optics, their positions must be controlled within 10^{-13} m rms. To keep a cavity resonant ('locked'), the most intuitive way is to look at the transmitted/reflected power and keep it maximal/minimal. However, the dependence of the power on the length near the resonance is quadratic: the sensitivity is poor and, above all, the signal is symmetric on both sides of the resonance, so the servo cannot immediately tell which way to actuate.

With the Pound–Drever–Hall locking technique [6] the light is modulated in phase using electro-optic crystals as explained in the previous paragraph. The modulation frequency is such that the sidebands are anti-resonant in the 3 km long Fabry–Perot cavities. They are reflected by the front mirror, whereas the resonant carrier probes the end mirror. A fraction of the carrier is reflected by the cavity and interferes with the sidebands at the modulation frequency. If this signal is demodulated with the right phase, we obtain an error signal that crosses zero at resonance. The signal is linear with deviation from resonance and therefore it is a good error signal.

The Pound–Drever–Hall technique is used for length sensing and control (LSC), but also for controlling angular motion by the wavefront sensing system as is done for the alignment control of the suspended injection bench and suspended input mode cleaner.

3. Virgo injection system

The Virgo injection system consists of four main elements: the laser system, the beam monitoring system (reduction of laser

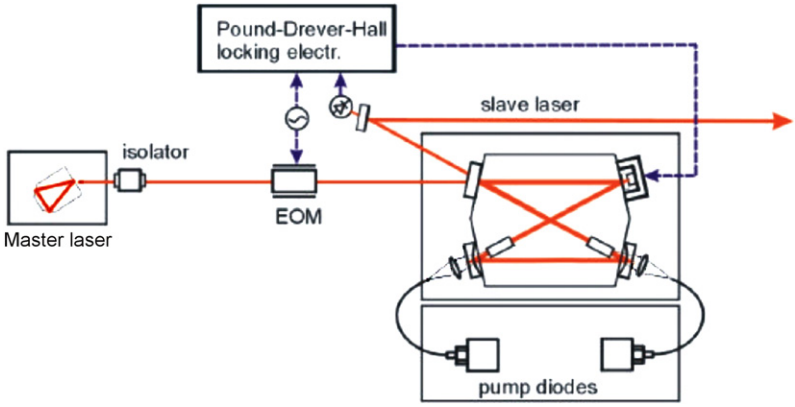

Figure 2. The Virgo laser based on the injection locking technique: the master is an innolight NPRO laser (single frequency) and the slave laser contains two Nd:YVO_4 rods pumped by fibre-coupled diodes. The injection-locking technique uses a 14 MHz phase modulator (EOM).

beam jitter at low frequency before the input mode cleaner), the input mode cleaner (laser beam spatial and spectral filtering) and the suspended injection bench (the bench in vacuum that enables the coupling of the light into the input mode cleaner and the matching of the laser beam into the interferometer by means of a parabolic telescope).

3.1. The laser source: an ultra-stable single-mode high power laser

For the laser system which requires a very powerful and stable laser, it has been chosen to injection-lock a high power monomode laser (slave laser) with a low power master oscillator. Injection locking is a well-known technique [7] to capture all the power of a multifrequency high power laser into a single-frequency output without any loss of power. With this technique we can also transfer the frequency stability and the amplitude stability of the master laser to the slave laser.

The master laser is a commercial innolight Mephisto 1000NE Nd:YAG laser which is able to deliver a 1 W-continuous monomode laser beam with a full width at half-maximum lower than 1 kHz. The relative intensity noise is about -150 dB Hz^{-1} in noise eater mode.

The slave laser is a 20 W single transverse mode neodymium–vanadate (Nd:YVO_4) ring laser (see figure 2) and has been developed by Laser Zentrum Hannover (LZH). The laser crystals are pumped longitudinally. The pump energy is delivered from fibre-coupled laser diodes. In stand-alone operation the laser oscillates in multiple longitudinal modes and emits two beams in opposite directions.

Two mirrors of the slave are mounted on piezo-transducers in order to allow us to compensate for external acoustic and mechanical perturbations. In order to keep the slave laser in the locking range relative to the master laser frequency, the length of the former one is controlled using the Pound–Drever–Hall locking technique.

The phase of the master is modulated at 14 MHz using a $LiNbO_3$ phase modulator. Assuming that the carrier is close to the resonance of the slave laser cavity, the light reflected by the slave contains a 14 MHz beat note between the reflected non-resonant sidebands and the slave oscillation, which is phase-shifted from the master carrier by ϕ [8]. Then, the amplitude of the 14 MHz beat note is proportional to ϕ and the demodulation gives an error signal that is sent to the electronic servo system feeding the two piezo-transducers of the slave.

These piezo-transducers enable the compensation of frequency shifts in the slave cavity. The first one yields a frequency correction sensitivity of 5 MHz V^{-1}, a servo bandwidth from DC to several kHz and a frequency shift up to 12 GHz. The second one (the fast one) yields a frequency correction sensitivity of 360 kHz V^{-1}, a bandwidth of 100 kHz and a frequency shift up to 10 MHz.

The unity gain frequency (UGF) for the overall servo loop is 100 kHz. The frequency noise of the laser follows the rules $10^4/f\,\mathrm{Hz}/\sqrt{\mathrm{Hz}}$ and the relative intensity noise at this level is 0.5×10^{-6} $\mathrm{Hz}^{-1/2}$ at 10 Hz and 10^{-6} $\mathrm{Hz}^{-1/2}$ at 100 Hz.

The laser frequency is pre-stabilized using the input mode cleaner cavity as a reference. The low frequency stability is achieved by an additional control system that stabilizes the IMC length below 15 Hz to the length of a rigid reference cavity (RFC) [9].

3.2. Beam monitoring system (BMS), IMC and SIB automatic alignment

In order to send the laser beam through the interferometer, we use an in-vacuum suspended bench which has two purposes: to clean spectrally and spatially the laser beam by means of a suspended triangular cavity, called the input mode cleaner (IMC), and to adapt the laser beam size to the interferometer to maximize the coupling efficiency. The beam monitoring system (BMS) is used to keep the laser beam in a fixed position before entering into the suspended injection bench (SIB), while the injection bench automatic alignment system is used to keep the input mode cleaner cavity locked and to avoid a drift of the suspended injection bench.

3.2.1. Beam monitoring system. Before entering the tower, two quadrant photodiodes (BMS_QN and BMS_QF) and four piezo actuators are used to keep the beam in a reference position (cf figure 3). This system permits the lowering of the beam jitter at low frequency and keeps the beam in a given reference position (a typical value is 1 μrad $\mathrm{Hz}^{-1/2}$ at 1 Hz).

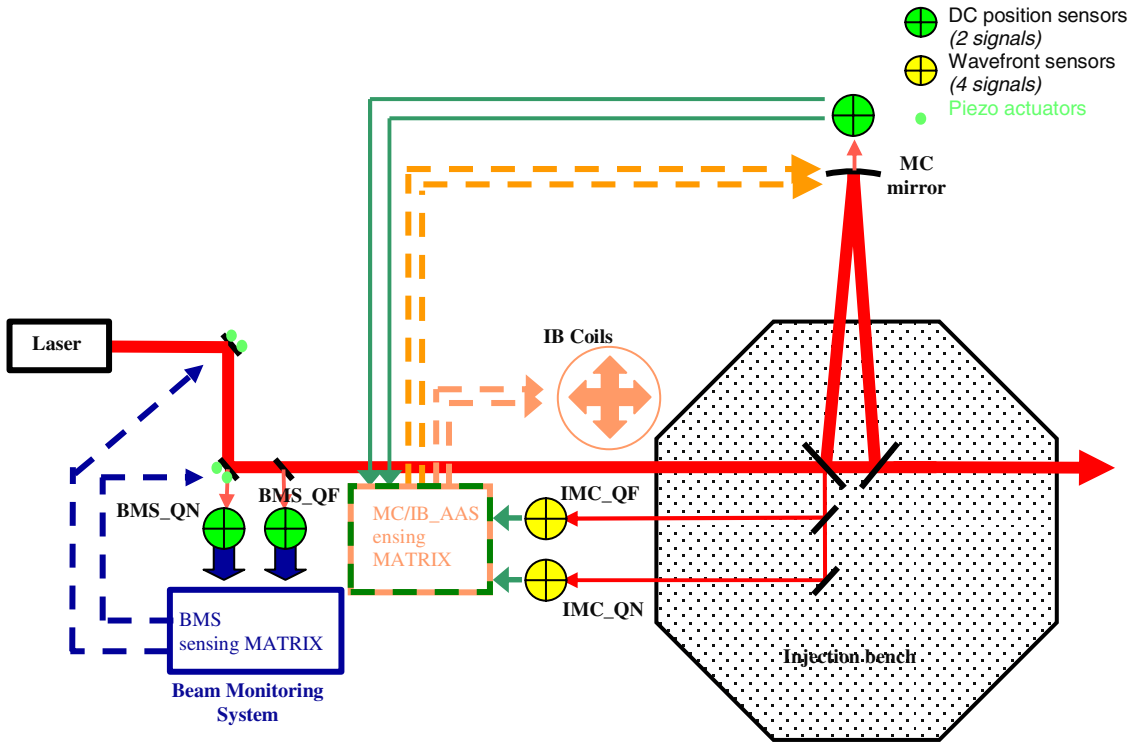

Figure 3. Beam monitoring system and injection system automatic alignment: piezo actuation is used for BMS corrections and coil-magnet control is used to control the injection bench and IMC position.

The unity gain of the loop is around 1 Hz. It also serves as a good monitor of the beam jitter noise before the input mode cleaner.

3.2.2. Input mode cleaner. This is a 287 m (round-trip) long suspended triangular cavity that aims to spatially filter the laser beam before it enters the interferometer. It also reduces the laser frequency and power fluctuations; a triangular geometry has been chosen in order to avoid back-reflection of the light in the laser [10].

In order to couple the maximum light in the interferometer recycling cavity it is necessary to spatially filter the laser beam to have a TEM_{00} spatial distribution of this beam. In fact, beam distortions are created by the optical components (such as electro-optical modulators) which are on the light path between the laser and the input mode cleaner.

The input mode cleaner behaves as a first-order low-pass filter for the power and frequency fluctuations of the incoming laser beam. The fluctuation suppression factor is given by

$$H(f) = \frac{1}{\sqrt{1 + \left(\frac{f}{f_0}\right)^2}} \tag{1}$$

where f_0 is the input mode cleaner cavity pole ($f_0 = c/4LF$, L: cavity half-round-trip length and F: cavity finesse).

For Virgo, $L = 143.5$ m and $f_0 = 508$ Hz.

Amplitude and frequency fluctuations of the incoming beam are suppressed as $1/f$ above the cutoff frequency f_0.

Using the beam monitoring system quadrant diodes to measure the beam jitter before the input mode cleaner, it is estimated that the angular beam motion was lower than $2 \times 10^{-2} \mu\mathrm{rad\ Hz}^{-1/2}$ between 1 Hz and 10 kHz.

As higher-order modes are suppressed by the input mode cleaner, beam jitter is decreased by a factor that is given by the following expression (assuming that the mode cleaner is much more stable than the beam because it is suspended):

$$A_S = \sqrt{\frac{T_{mn}}{T_{00}}} = \sqrt{\frac{1}{1 + \left(\frac{2}{\pi} F \sin\left(\frac{2\pi \Delta\upsilon_{mn}}{c} L\right)\right)^2}} \tag{2}$$

where A_S is the ratio between higher-order mode amplitude and the fundamental mode (it corresponds to the inverse of the jitter amplitude attenuation factor); $\Delta\upsilon_{mn} = \frac{c}{2L}(m + n)\frac{1}{\pi}\arccos\sqrt{g}$ and $g = 1 - L/R_C$; R_C is the end mirror curvature radius.

The filtering efficiency depends on the factor $\frac{2}{\pi}F \sin(\frac{2\pi\Delta\upsilon_{mn}}{c}L)$ which has to be as high as possible for the lower-order modes, in order to minimize the beam jitter.

To satisfy this condition F has to be as high as possible and the input mode cleaner has to be non-degenerate, i.e. $(m + n)\arccos\sqrt{g} \neq n\pi$ (n is an integer).

3.2.3. Injection bench and IMC automatic alignment. Six degrees of freedom (dof) are controlled, four for the injection bench (θ_x, θ_y, θ_z and z) and two for the MC (θ_x, θ_y).[15]

IB and MC dof are controlled with a mix of optical-lever-based DC controls, using the position of the beam read

[15] For the suspended injection bench and input mode cleaner, the x direction is along the interferometer axis, the y direction is the vertical direction and the z direction is along the input mode cleaner axis.

by a quadrant photodiode located after the MC end mirror (figure 3), and four interferometric signals (Ward signals: for a single Fabry–Perot cavity the alignment control signals can be derived from the reflection from the cavity using the wavefront sensing method [11]) using two wavefront sensors (IMC_QN and IMC_QF in figure 3). The performance of this system enables the control of all the angular degrees of freedom within ± 0.5 μrad, with a unitary gain frequency (UGF) of about 1 Hz for all the degrees of freedom except the injection bench z that has a very low UGF.

4. Virgo detection system

The light exiting the interferometer at the output port is optically filtered using an output mode cleaner (OMC). The OMC is a short rigid triangular cavity made from a piece of silica properly polished and coated [12]. This cavity has an optical length of about 2.5 cm and a finesse of 50. Once filtered, the light is split over an array of three InGaAs photodiodes. These are 3 mm diameter photodiodes (specially developed by Hamamatsu) with quantum efficiency greater than 90%.

Their arrangement allows the easy adaptation of the number of used photodiodes to the dark fringe power (each photodiode can manage up to 100 mW). The current flowing in each photodiode is pre-amplified before being synchronously detected at the main modulation frequency (6.26 MHz). One per cent of the dark fringe light is extracted before it enters the output mode cleaner (B1p beam in figure 1) and detected, in order to help the interferometer lock acquisition process. The light reflected by the second face of the beamsplitter (B5 beam in figure 1) is also gathered and used for interferometer control purposes. The reflection of the interferometer (B2 beam) is also used to control some interferometer degrees of freedom. Similar photodiodes detect the two beams transmitted through the two end mirrors (B7 and B8). Also placed at all these output ports are the quadrant photodiodes used for automatic alignment [13] purposes and the CCD cameras that are used to help in the interferometer pre-alignment.

Once the interferometer is locked on the dark fringe, the output mode cleaner length should be locked to the laser wavelength in order to have it resonant with the TEM00 mode. To achieve this, the output mode cleaner optical length is varied by scanning its temperature and the transmitted beam is monitored by a digital CCD camera. The camera image is read by a real time CPU that continuously compares the beam shape with the expected TEM00 mode. The image is processed 10 times per second and a χ^2 variable is calculated at this rate. As the χ^2 variable becomes smaller than a user-defined threshold, the output mode cleaner control system tries to lock it to the resonance. Typically the lock attempt is started when the transmitted power is about 15% of the power at the resonance. In order to get an error signal, the OMC length is modulated at 28 kHz using a piezoelectric actuator. The error signal is synchronously detected at this same frequency by demodulating the current flowing in the photodiode placed on the transmitted beam and is used to adjust the temperature of the cavity. This is achieved by means of a digital feedback also running at 10 Hz and with a unity gain of around 20–30 mHz.

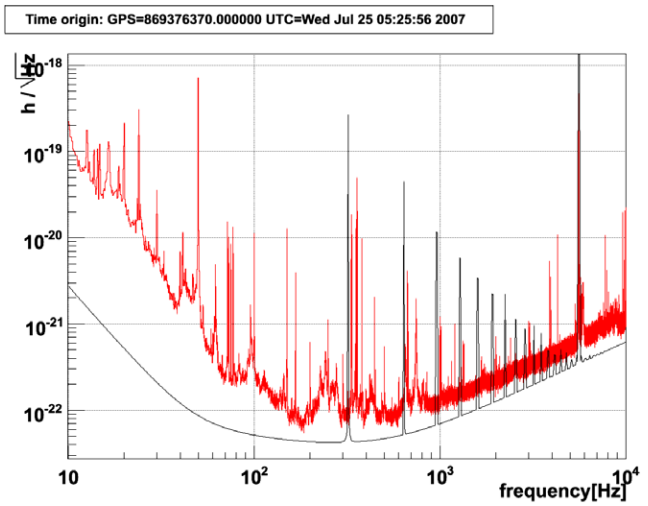

Figure 4. Recent Virgo sensitivity curve compared with Virgo design sensitivity (smooth curve).

5. Current performance and mid-term evolution

The main performance of the apparatus is characterized by the sensitivity curve of the instrument (see figure 4). This sensitivity is limited by different sources of noise [14] depending upon the bandwidth. At low frequencies (below 100 Hz), the sensitivity is limited essentially by 'control noises' (angular and longitudinal). In the middle frequency range (100–1000 Hz), the limiting noises are environmental noises coupled by various sources of diffused light. Finally above 1 kHz, the sensitivity is shot-noise-limited.

Virgo is currently facing two major problems in terms of sensitivity performance: diffused-light-related noises and input power limitation due to thermal lensing effects. Many activities have already started to overcome these limitations and will continue after the scientific run.

Regarding the diffused light, we are facing three different topics: the transmission of the far end mirrors, the dark port and the reflection port of the interferometer. In each case, some light from the main beam is back-scattered and acts as a vector, which couples the environmental noise (acoustic and seismic) to the interferometer output, limiting the sensitivity in various spectral regions between 10 Hz and 1 kHz. The work of mitigation is being done by trying to decrease the environmental noise sources and, at the same time, by improving diffused light problems, substituting some optics with bigger and better quality ones, as well as by dumping all spurious beams present at the different interferometer ports.

As a consequence of the thermal effects observed in Virgo [15], which have already been described for other large interferometers [16], the interferometer is being run with 8 W at the input instead of the 10 W that could be delivered at the output port of the input mode cleaner.

This has been shown to be an experimental limit. Beyond this limit, the resonance properties of the sideband fields (mandatory to build the Pound–Drever signals used to control the length of the cavities) in the recycling cavity are changed in

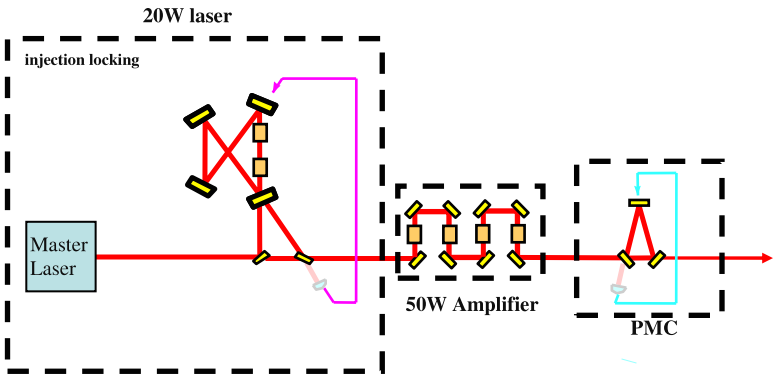

Figure 5. Power enhancement of Virgo laser: Virgo 20 W injection-locked laser amplified by a four-stage amplifier with a pre-mode cleaner (PMC).

such a way that the longitudinal control of the optical cavities becomes unstable.

The phenomenon can be explained as follows: the input mirrors of the Fabry–Perot cavities are absorbing some energy (typically, 0.7 ppm cm^{-1} for the substrate and 1.2 ppm for the coating, but the current estimation gives losses that are 10 times higher). As the temperature of the mirror is changed in a spatially non-uniform way, the refractive index of the material is changed in a proportional way, creating a virtual lens in the recycling cavity.

The sidebands, which are resonating only in the recycling cavity (and not in the FP arm cavities like the carrier), are then degenerated in higher-order modes, which have different resonance properties. Since we are already using optics with the lowest available absorption, the only solution is to implement a thermal lensing compensation system. A concept based on the systems already running in equivalent experiments (LIGO, GEO) is currently being developed and should be integrated at the beginning of 2008. It consists of a CO_2 laser focused on the mirror in a ring shape that is designed to make the temperature uniform in the substrate.

6. Virgo+: a first upgrade to Virgo

6.1. Description

Before reaching a second generation of interferometers, in order to enhance the sensitivity by a factor of 10 with respect to the first generation, there is the possibility to perform minor upgrades and thus improve significantly the sensitivity of the detector. The list of these modifications has been gathered under the project name 'Virgo+'.

From the optical point of view, Virgo+ should improve the shot noise which is limiting sensitivity at the high and middle frequency regions by means of an increase of the interferometer input power up to 30 W.

To obtain this goal, assuming a typical 60% transmission of the input mode cleaner, there is the need to amplify the current 20 W laser source to 50 W. This will be achieved through a four-stage Nd:YVO_4 amplifier provided by Laser Zentrum Hannover (LZH). This amplifier is currently being tested. A power of 64 W at the output port of the amplifier has been achieved on a test bench. In this configuration it has been demonstrated that we can have more than 50 W of power at the output port of the pre-mode cleaner.

The pre-mode cleaner cavity, a triangular 13 cm half-round-trip long cavity (finesse = 500) made of Zerodur and installed in a vacuum tank, will be devoted to filtering out the amplitude fluctuations of the laser. The main scheme of the Virgo+ laser system is given in figure 5.

Finally, an improved sensitivity will be obtained through the enhancing of the power stored in the interferometer by increasing the finesse of the Fabry–Perot cavities up to 150 (current finesse is 50).

These changes will probably induce some strong thermal effects in the Faraday isolator (located on the suspended injection bench) and also at the level of the input mirrors of the 3 km Fabry–Perot cavities. Concerning the Faraday isolator, we are currently studying the possibility of passively compensating for thermal lensing by adding a small piece of crystal in which the thermal lensing effect is opposite to that experienced by the TGG crystal (magneto-optic crystal used in the Faraday isolator).

For the thermal lensing in the long cavity input mirrors, as previously explained, the correction system consists of projecting a CO_2 light ring onto the input mirrors to render uniform the temperature in the substrate and on the coating.

6.2. Noise budget and performances of Virgo+

With the Virgo+ upgrade the sensitivity could be increased by a factor of 2–4 with respect to the Virgo design, depending on the frequency region (see figure 6). The commissioning phase for Virgo+ should start in 2008 and end in 2009, with the start of a science data-taking period in parallel with the equivalent American detector LIGO.

The figures of merit, which are used for coalescing binary sources (two kinds of coalescing binary signals are considered: a pair of neutron stars, each of 1.4 solar masses and a pair of 10 solar mass binary black holes) [17] are the following:

First, the *Sight Distance@SNR* = 8, is the maximum distance at which an optimally oriented source would be detected with a signal to noise ratio (SNR) = 8.

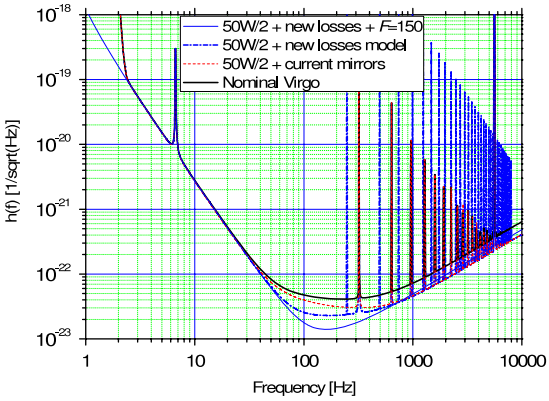

Figure 6. Virgo+ design sensitivity (considering that we have 25 W entering the ITF) for a Fabry–Perot finesse of 50 with current Virgo mirrors (dashed line), with new low-loss mirrors (dashed–dotted line) and with new low-loss mirrors and a finesse of 150 (best curve between 50–700 Hz, thinnest line). The thickest line is the Virgo design sensitivity.

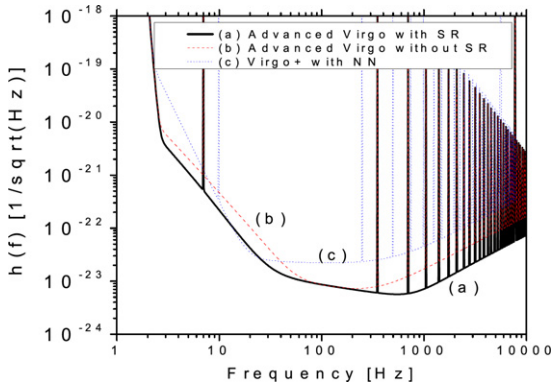

Figure 7. Preliminary Advanced Virgo design sensitivity assuming an input power of 100 W, a mirror weight of 40 kg, a recycling gain of 50 and a Fabry–Perot finesse of 600.

Table 1. Expected event rates at SNR = 7 as a function of the sight distance D in megaparsecs (averaged over the relative source–detector orientation).

D (Mpc)	Event rate@SNR7 (yr^{-1})
10	3.44×10^{-3}
15	2×10^{-2}
20	3.00×10^{-2}
30	6.44×10^{-2}
40	1.21×10^{-1}
50	2.20×10^{-1}
70	7.08×10^{-1}
100	1.63
150	2.30
200	5.44
300	18.4

Then, the $Events/Year@SNR = 7$ is the rate of events expected, assuming a conservative estimate of source density, and averaging over the geometrical parameters.

It is something of a nuisance that the two parameters refer to different SNR. The reason is that the theoretical estimates for the event rates are typically made using SNR = 7, while other experiments (such as LIGO) use SNR = 8 for the sight distance.

With the current Virgo sensitivity ($D = 5$ Mpc), we expect 1 event every 2000 years which is very low; this is why upgrades are necessary to develop gravitational wave astronomy. Table 1 shows the expected event rates with a SNR = 7 as a function of the sight distance, also called the horizon of the detector.

7. Advanced Virgo

Even if a first detection is possible, the present sensitivity of Virgo and LIGO will not be sufficient to detect more than 0.1 events per year. For this reason it is important to prepare the upgrades of the present detector, considering that, for a uniform distribution of sources, an increase of the sensitivity by only a factor of 2 will increase the expected event rate by about a factor of 2^3.

The first goal of advanced Virgo is to enhance the sensitivity by a factor of 10 with respect to the current Virgo design sensitivity; this should increase the rate of detectable events by a factor of 1000.

The main upgrade of advanced Virgo will be the increase of the input power up to 200 W. Already, LZH is working on a 200 W amplification module to be added to the optical path that could amplify a single-mode single-frequency laser up to 200 W with a multiple-stage Nd:YVO_4 amplifier. There is also the possibility to recycle the signal using a signal recycling mirror (SR). As can be seen in figure 7, with this configuration we should significantly improve the sensitivity of the detector between 3 and 50 Hz and above 300 Hz.

Such high power will induce some thermal lensing and birefringence problems in the optical components, such as polarizers, Faraday isolators and electro-optical modulators. In order to study these effects and compensate them, a research and development program has been put in place.

Within the VIRGO collaboration, a huge effort is being made in order to implement an all-fibred system for the advanced Virgo injection system. In particular, there is the possibility to replace the input mode cleaner cavity with an optical fibre and to use an all-fibred laser source providing a single-frequency 200 W. This kind of laser has already been demonstrated experimentally [18].

The main issues deriving from the higher power will be thermal effects. Side effects will concern the increase in scattered light.

8. Conclusion

The large-scale, power recycled Michelson interferometer, Virgo, has been presented mainly from the point of view of the different optical systems that are used, such as the laser system, the injection system and the alignment control of the interferometer.

The current Virgo configuration needs to be upgraded in order to increase the probability of gravitational wave detection. The first step is the so-called Virgo+ project which

has as its main goal the increase in laser power and Fabry–Perot arm finesse up to 150 in order to improve the sensitivity of the detector between 100 Hz and 10 kHz by a factor of 2. The second step, planned for the next decade, should improve the Virgo sensitivity by a factor of 10 and, as a consequence, the rate of detectable events by a factor of 1000. This should be the real starting point for gravitational wave astronomy.

References

[1] Acernese F *et al* 2007 The Virgo interferometric gravitational antenna *Opt. Lasers Eng.* **45** 478–87

[2] Braccini S *et al* 2005 Measurement of the seismic attenuation performance of the Virgo superattenuator *Astropart. Phys.* **23** 557–65

[3] Sigg D *et al* 2002 Commissioning of the LIGO detectors *Class. Quantum Grav.* **19** 1429–35

[4] Ando M *et al* 2002 Current status of TAMA *Class. Quantum Grav.* **19** 1409–19

[5] Willke B *et al* 2002 The GEO 600 gravitational wave detector *Class. Quantum Grav.* **19** 1377–87

[6] Drever R W, Hall J L, Kowalski F V, Hough J, Ford G M, Munley A J and Ward H 1983 Laser phase and frequency stabilization using an optical resonator *Appl. Phys.* B **31** 97

[7] Siegman A E 1986 *Lasers* (University Science Books)

[8] Barillet R *et al* 1996 An injection-locked ND:YAG laser for the interferometer detection of gravitational waves *VIRGO Internal Note* VIR-NOT-LAS-1390-010

[9] Bondu F *et al* 1996 Ultrahigh spectral purity laser for the Virgo experiment *Opt. Lett.* **21** 582–4

[10] Rudiger A *et al* 1981 A mode selector to suppress fluctuations in laser beam geometry *Opt. Acta* **28** 641–58

[11] Morrison E, Meers B J, Robertson D I and Ward H 1994 Automatic alignment of optical interferometers *Appl. Opt.* **33** 5041–9

[12] Flaminio R *et al* 2002 Interferometer signal detection system for Virgo experiment *Class. Quantum Grav.* **19** 1857–63

[13] Babusci D *et al* 1997 Alignment procedure for the VIRGO interferometer: experimental results from the Frascati prototype *Phys. Lett.* A **226** 31–4

[14] Tournefier E *et al* 2007 Noise budget and noise hunting in Virgo, gravitational waves and experimental gravity *Proc. Rencontres de Moriond 2007 (La Thuile, March 2007)*

[15] Laval M 2007 Modeling of thermal effects in Virgo, Gravitational waves and experimental gravity *Proc. Rencontres de Moriond (La Thuile, March 2007)*

[16] Winkler W *et al* 1991 Heating by optical absorption and the performances of gravitational waves detectors *Phys. Rev.* A **44** 7022–36

[17] Flaminio R *et al* 2005 Advanced Virgo white paper *VIR-NOT-DIR-1390-304* November

[18] Jeong Y *et al* 2004 Single-frequency polarized ytterbium-doped fiber MOPA source with 264 W output power *Conf. on Lasers and Electro-Optics, 2004 (CLEO) (16–21 May 2004)* volume 2 1065–6